

Control of Separated Flow by a Two-Dimensional Oscillating Fence

J. J. Miao,* K. C. Lee,† M. H. Chen,† and J. H. Chou‡
National Cheng-Kung University, Tainan, Taiwan 70101, Republic of China

Control of separated flow behind a backward-facing step using a two-dimensional oscillating fence installed upstream has been investigated in this work. Parameters of the flow considered included the reduced frequency of the oscillating fence, the distance from the oscillating fence to the backward-facing step, the ratio of the maximum height of the oscillating fence to the step height, and the Reynolds number. It was found that with the experimental parameters properly selected the time-mean reattachment length of the separation region could be reduced over 40%, compared to the case without the presence of an oscillating fence. The evolution of unsteady flow behind a backward-facing step was further studied in detail by a phase-averaging measurement technique. The results obtained indicate that suppression of the separated flow behind the step is mainly due to the downwash motion induced by the vortical structure released upstream from the oscillating fence, when it convects over the step.

Nomenclature

f	= frequency of the oscillating fence
h	= instantaneous height of the fence
h_f	= maximum height of the fence
h_s	= height of backward-facing step, = 1.5 cm
I_r	= intermittency function defined in Eq. (2)
K	= reduced frequency, = fh_f/U_0
K_{cr}	= critical reduced frequency, above which organized vortical structure develops behind the oscillating fence as it extends into the flow
L_s	= distance from the oscillating fence to the step
Re_θ	= Reynolds number, = $U_0/\theta\nu$
t	= time
T	= time period of the oscillating motion of the fence
U, u	= time-mean streamwise velocity and streamwise velocity fluctuation
U_0	= freestream velocity measured at the inlet of the test section
U_a	= streamwise growth rate of the vortical flow structure behind the oscillating fence
X	= streamwise coordinate
X_r	= time-mean reattachment length of the separated flow behind the backward-facing step, without the presence of the oscillating fence, but with a square-wave trip upstream
X'_r	= time-mean reattachment length of the separated flow behind the backward-facing step measured
Y	= vertical coordinate
Z	= spanwise coordinate
θ	= boundary-layer momentum thickness measured at the step, without the presence of the oscillating fence
ν	= kinematic viscosity of air
ϕ	= phase angle of the oscillating motion of the fence
Ω_z	= time-mean vorticity in the Z direction
$-$	= time-mean quantity
$\langle \rangle$	= ensemble-averaged quantity
ΔX_r	= the reduction of the time-mean reattachment length measured, = $X'_r - X_r$

Introduction

CONTROL of separated flow using unsteady means, for its immediate applicability to engineering problems and fruitfulness in the physical phenomena involved, has become an active research area in fluid mechanics. In earlier works^{1,2} the present authors considered the flow of a two-dimensional oscillating fence immersed in a flat-plate turbulent boundary layer and found that an organized vortical structure could be produced by the oscillating fence if its reduced frequency is higher than a critical value $K_{cr} = 0.009$. This finding introduces the possibility that this flow characteristic might be utilized to enhance the momentum exchange between the flow near the wall and the freestream fluid; hence, the flow separation phenomenon, if it originally occurred downstream, could be suppressed. In the present work this possibility was further explored by installing a two-dimensional oscillating fence upstream of a separation region, and its effectiveness was evaluated.

The separated-flow configuration selected for the present study is an ordinary backward-facing step. This flow, by nature having the separation point fixed at the step, is frequently regarded as a basic model of separated flows.^{3,4} A fair number of works on this flow have been reported in the literature³ that conveniently provide references for the present results to be compared with.

A number of methods for suppressing the separated flow behind a backward-facing step have been proposed in the literature. Roos and Kegelman⁵ proposed a concept of enhancing the momentum transfer in the separated shear layer by introducing a harmonic disturbance of small amplitude at the location of the step. They found that the separation region could be reduced by more than 30%. Koga⁶ attempted an idea of installing an oscillating flap in the zone of flow separation; thus, the unsteady flow structure generated could effectively convect the low-speed fluid downstream. As found, the time-mean reattachment length could be reduced by more than 60%, provided that the oscillating flap was installed properly.

To be somewhat different from the previous ideas, the present work is intended to place a vertically oscillating fence upstream of a backward-facing step. Our viewpoint was that the unsteady vortical structure released from an oscillating fence¹ would interact with the flow behind the backward-facing step; consequently, the separation region could be suppressed. The effectiveness of the oscillating fence employed should depend on its geometrical parameters and reduced frequency. Thus, in this work experiments were made to correlate the reduction of the reattachment length with the con-

Received Nov. 8, 1989; revision received April 9, 1990; accepted for publication July 5, 1990. Copyright © 1991 by the American Institute of Aeronautics and Astronautics, Inc. All rights reserved.

*Associate Professor, Institute of Aeronautics and Astronautics, Member AIAA.

†Graduate Student, Institute of Aeronautics and Astronautics.

‡Professor, Department of Engineering Sciences.

trolling parameters. Moreover, velocity measurements that were assisted by a phase-averaging technique were performed to study the evolution of the unsteady flow. The results obtained further shed light on the physical mechanisms involved in the interaction of the unsteady vortical structure and flow behind a backward-facing step.

Experimental Facility

Experiments were performed in a low-speed closed-type wind tunnel, whose test section is 15×15 cm in cross section. An aluminum sheet of 0.2 mm thickness and 15 cm width was inserted into the test section wall and driven in a sinusoidally oscillating motion. The maximum amplitude of the oscillating motion h_f was adjustable in a range between 0 and 2 cm. This piece of aluminum will be called the "fence" in this paper. Downstream of the fence, a backward-facing step was arranged in such a way that its height and distance to the oscillating fence could be varied in accordance with experimental needs.

In this study the height of the backward-facing step h_s was fixed at 1.5 cm. Thus, the aspect ratio of the step, i.e., the spanwise width vs the height, is 10, ensuring that flow along the centerline of the step is basically two-dimensional.⁷ It was found that the two-dimensionality of the flow was greatly improved with the insertion of the oscillating fence.⁸ In this study most of the velocity measurements were made along the centerline of the step.

The coordinate system employed for the present study is shown in Fig. 1, in which the notations describing the geometry of the flow configuration are given. Not shown in detail in this figure is that a square-wave trip device, 2 mm in height, was placed 2 cm downstream of the inlet of the test section. This resulted in the boundary-layer momentum thickness at the step θ to be comparable to the step height.

The experiments were performed at U_0 in a range of 0.5–11.4 m/s. Without the presence of the oscillating fence, the freestream turbulence intensity measured was about 0.5%. It was noted that the insertion of the oscillating fence introduced a periodic disturbance in the freestream. This variation also caused the pressure on the opposite wall to fluctuate sinusoidally. The pressure fluctuation level measured on the opposite wall was found to be about one-sixth of the level measured on the wall with the oscillating fence.⁸

The oscillating fence was driven by a servomotor, which was capable of producing an oscillatory motion with a frequency up to 20 Hz. The harmonic motion of the fence was described by

$$h = \left(\frac{h_f}{2}\right) (1 - \cos 2\pi f t) \quad (1)$$

Thus, the zero phase angle of the oscillatory motion was denoted to be the instant when the fence was completely

retracted into the wall. The phase information was obtained from an optical-electro sensing device,⁸ whose output signal was taken as the reference for the phase-averaging procedure.

The instantaneous, two-dimensional velocity measurements were performed with a cross-type hot-wire probe. In addition, a DANTEC split film was employed for the streamwise velocity measurements in the region where the reverse flow was possible. Either probe was mounted on a two-dimensional traversing mechanism, controlled by a 16-bit personal computer for automatic data acquisition.

A smoke-wire visualization technique was employed to assist our understanding of the flow. The smoke was generated by heating a stainless steel wire of 0.6 mm diam, on which a film of kerosene oil was coated. This wire was inserted vertically 3 cm away from the centerline of the test section and 3 cm upstream of the oscillating fence. The flow visualization experiments were performed at the freestream velocity below 2 m/s; thus, the Reynolds number based on the diameter of the wire was lower than 80. From the pictures taken it could be confirmed that vortex shedding from the wire was barely seen, compared to the large disturbances generated by the oscillating fence. The smoke was illuminated by a thin sheet of light produced by a 4-W argon-ion laser. Pictures were taken by a 35-mm camera whose shutter control was synchronized with the phase of the oscillating fence. However, due to the mechanical delay of the shutter, the phase at which the picture was taken might not exactly coincide with the desirable phase. This discrepancy became pronounced as the oscillating frequency was increased beyond 10 Hz. Most of the pictures were taken with an exposure time of 1/125 s.

Technique for Measuring Reattachment Length

It has been suggested that the reattachment point of the separated flow behind a backward-facing step can be taken at the location on the wall surface where the velocities measured in the reverse and forward directions are of equal probability.^{9,10} Detecting the reattachment point requires a technique that is capable of distinguishing the flow direction. In the preliminary experiments different techniques that might serve this purpose were attempted. These techniques include the methods employing a thermal tuft probe,⁹ a split film, and a yaw pitot tube, respectively.

It is interesting to note that the reattachment points determined by the three techniques do not coincide. The thermal-tuft measurement gives the reattachment length quite close to that obtained by other investigators³ for a backward-facing step with the same expansion ratio as the present flow. However, the pitot tube and the split film measurements give the reattachment lengths to be about 25% shorter. It is our view that the measurements obtained by the thermal tuft probe should be more reliable than those obtained by the other techniques, because the latter techniques introduce additional disturbance into the flow due to the physical presence of the probe.

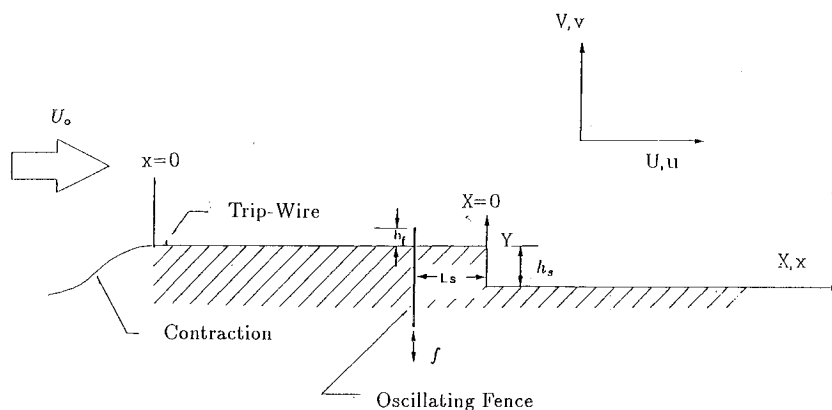


Fig. 1 Coordinate system.

However, the merit of the thermal-tuft technique was overshadowed by its inconvenience of moving continuously along the streamwise direction. In view of the fact that measurement of reattachment length in the present study was intended to be made for a large number of cases, we finally gave up this technique, and selected the technique using the split-film. We were aware of the inaccuracy that might have resulted from the split-film measurements. However, in the present study our main concern was the relative reduction of the reattachment length in comparison with X_r , the reattachment length

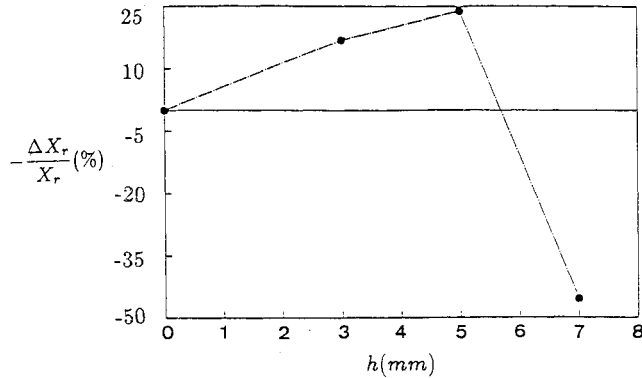


Fig. 2a Diagram of $-\Delta X_r/X_r$ vs the height of the two-dimensional plate, $L_s/h_s = 4$.

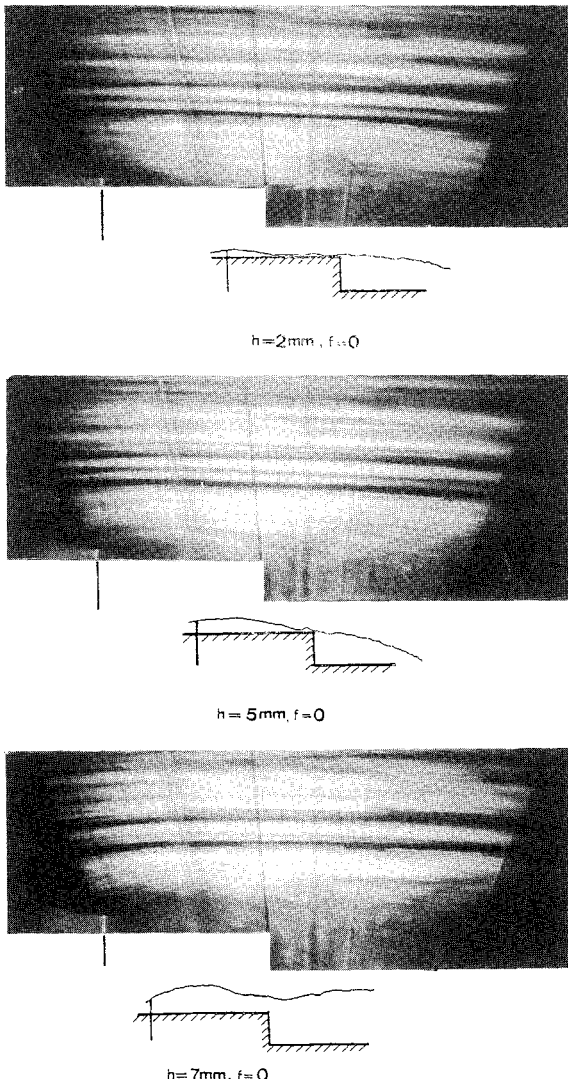


Fig. 2b Smoke visualization pictures for the cases of $h = 2, 5$, and 7 mm, respectively.

of an ordinary backward-facing step, with the square-wave trip situated upstream, obtained by the same technique. Thus, the inherent inaccuracy of this technique should not degrade the value of the results obtained.

The split-film probe distinguishes the flow direction by comparing the voltages measured from the heating sensors on two sides. The fraction of time corresponding to flow in the forward direction can be represented by an intermittency function I_r :

$$I_r = \sum_{i=0}^{N-1} [1 - H(i)] \Delta t / N \Delta t \quad (2)$$

where $H(i)$ is a step function, $H = 1$ represents the reverse flow situation, and $H = 0$ represents the forward flow situation. Thus, the reattachment point was determined to be the location where $I_r = 0.5$.

Measurements of Reattachment Length with the Fence Fixed Upstream

Before the experiments of a two-dimensional fence undergoing oscillatory motions were conducted, efforts were made to study the flowfield under the condition that the fence was fixed. The fence, with an adjustable height, was located at a streamwise location of $X = -4h_s$. It is interesting to point out that by inserting the fence at various heights the influences on the reattachment length of the separated flow behind the backward-facing step are remarkable. The trend is seen in Fig. 2a. When $h = 5$ mm, i.e., $L_s/h = 12$, the reduction of the reattachment length is pronounced. In terms of $-\Delta X_r/X_r$, the value obtained is about 25%. When $h = 7$ mm, the reattachment length increases, instead of reducing, $-\Delta X_r/X_r$ amounting to -50% . The geometrical ratios L_s/h corresponding to this rapid transition fall in a range of 9–12, which concurs with the distance required for a separated flow established behind a fence immersed in a flat-plate boundary layer to reattach to the wall.¹¹ This finding signifies that the reduction of the reattachment length strongly depends on whether the separated flow behind the fence reattaches or not before the step. Apparently, for the case of $h = 7$ mm the separated flow behind the fence does not reattach before the step; thus, the effective height of the backward-facing step increases.

Further evidence to support this reasoning can be seen from flow visualization pictures presented in Fig. 2b, which shows the pictures obtained with $h = 2, 5$, and 7 mm, respectively. For $h = 5$ mm the separated flow reattaches to the wall surface immediately upstream of the step and the streamlines in the freestream appear to continue curving toward the region behind the step. This situation corresponds to a nearly optimal reduction of the reattachment length.

Experimental Parameters

For the cases of a two-dimensional fence in oscillation, the parameters controlling the reattachment length of the separated flow behind the backward-facing step can be grouped into a functional form as

$$\Delta X_r = f(h_s, h_f, L_s, f, U_0, \theta, \nu) \quad (3)$$

where ΔX_r denotes the reduction of the reattachment length, which is the major quantity of interest in this work. It reflects the effectiveness of the present control mechanism. By a dimensional analysis, Eq. (3) can further be rearranged into the following form:

$$\Delta X_r/X_r = F(L_s/h_f, K, h_f/h_s, \theta/h_s, U_0\theta/\nu) \quad (4)$$

The physical significance of the first three parameters on the right-hand-side of Eq. (4) deserves further discussion, as follows.

The parameter L_s/h_f is proposed for the reason that the oscillating fence has to be installed at a proper distance up-

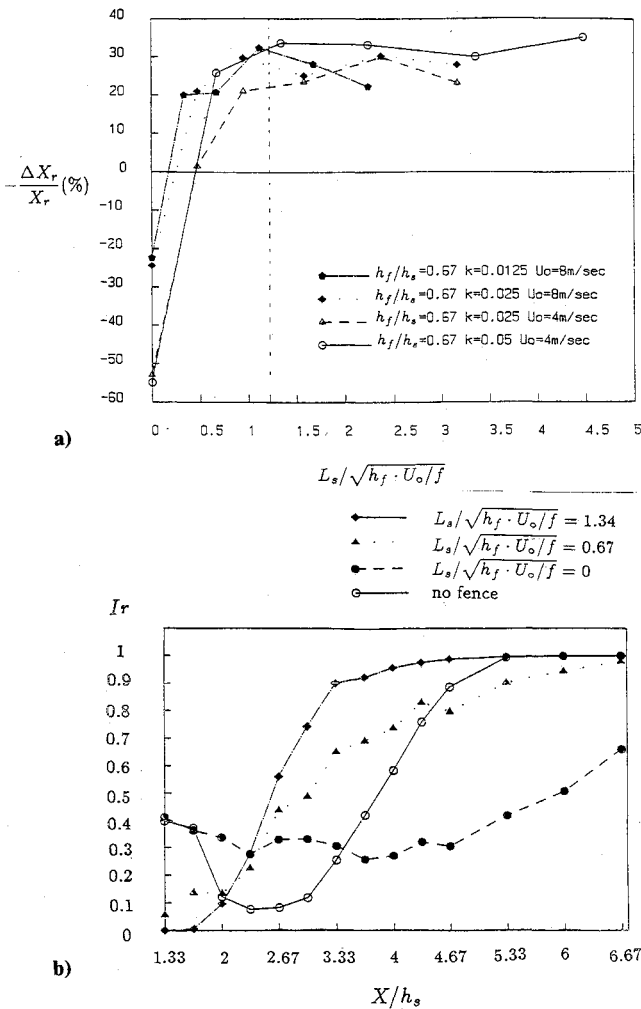


Fig. 3 Effect of $L_s/\sqrt{(h_f U_0)}/f$: a) $-\Delta X_r/X_r$ vs $L_s/\sqrt{(h_f U_0)}/f$; b) intermittency distributions for $L_s/\sqrt{(h_f U_0)}/f = 1.34, 0.67$, and 0 , respectively, at $(K, h_f/h_s, U_0) = (0.05, 0.67, 4 \text{ m/s})$.

stream of the step, so that the unsteady separated flow generated by the oscillating fence may effectively suppress the separation region behind the backward-facing step. The selection of L_s can be considered from two standpoints. If the reduced frequency K is small, i.e., the separated flow produced by the oscillating fence behaves quasisteadily, L_s is required to be larger than $9h_f$, learned from Fig. 3. On the other hand, if K is larger than $K_{cr} = 0.009$, corresponding to a situation that the unsteady vortical structure develops behind the oscillating fence,¹ L_s should be greater than a length equivalent to the time-averaged streamwise growth rate of the vortical structure multiplied by half the oscillating period. Thus, the vortical structure can be accommodated in a streamwise region upstream of the step when the fence extends into the flow. According to the physical model proposed by Miao et al.,¹ the time-mean growth rate of the vortical structure at $K > K_{cr}$ is suggested to be $U_0/2$, independent of K . However, from the experimental data given by Francis et al.¹² and Reynolds and Carr,¹³ one finds that the growth rate proposed by Miao et al.¹ actually corresponds to a limiting case as K approaches 0.1 , which is an order higher than the K values of interest in the present study. Therefore, for the cases of K in a range between 0.01 and 0.1 , one adopts an empirical relation proposed by Francis et al.¹² and Reynolds and Carr¹³ that the normalized time-mean growth rate of the vortical structure behind an oscillating fence U_a/U_0 is proportional to \sqrt{K} . That is,

$$U_a/U_0 = 2.44\sqrt{K} \quad (5)$$

Consequently, L_s should be chosen as

$$L_s > U_a \cdot \frac{T}{2} = 1.22 \sqrt{\frac{h_f U_0}{f}} \quad (6)$$

Here, it is seen that $\sqrt{(h_f U_0)/f}$ is a length scale appropriate for normalizing L_s , when $0.01 < K < 0.1$.

The reduced frequency K , i.e., $(h_f/f)/U_0$, indicates a ratio of the characteristic velocity of the oscillating fence to the freestream velocity. Considering that the present purpose is to accomplish an effective control on the separated flow downstream, we therefore emphasize the cases of K larger than the critical value, $K_{cr} = 0.009$ (Ref. 1). When K is greater than K_{cr} , the oscillating fence is capable of producing organized vortical structures.

The geometrical parameter h_f/h_s signifies a comparison of the vertical size of the unsteady vortical structure produced by the oscillating fence and the vertical size of the separated flow behind the backward-facing step. In this study we focused on the cases in which this parameter was of order 1.

Under the present experimental conditions the fourth parameter on the right-hand side of Eq. (4), θ/h_s , varied in a range of 0.7 – 1 , depending on U_0 . However, this parameter was not studied independently in this work, which would have required boundary-layer trips of different heights while the Reynolds number was held constant.

Experimental Results

Effect of $L_s/\sqrt{(h_f U_0)}/f$

Regarding the effect of $L_s/\sqrt{(h_f U_0)}/f$ on $-\Delta X_r/X_r$, the data collected from four series of experiments of which the K values are greater than 0.009 are plotted in Fig. 3a. These distributions consistently show that, as $L_s/\sqrt{(h_f U_0)}/f$ increases over 1.22 , the $-\Delta X_r/X_r$ values are weakly dependent on this parameter, where the variations in each of distributions are within a band of $\pm 5\%$ in value. When $L_s/\sqrt{(h_f U_0)}/f$ is less than 1.22 , $-\Delta X_r/X_r$ varies in a much more drastic fashion. The $-\Delta X_r/X_r$ value decreases below zero as $L_s/\sqrt{(h_f U_0)}/f$ approaches zero. Furthermore, when $L_s = 0$, the values of $-\Delta X_r/X_r$ obtained vary with the freestream velocity U_0 . This appearance suggests that, when $L_s/\sqrt{(h_f U_0)}/f$ approaches zero, the parameter of the Reynolds number may play a role affecting the flow characteristics. However, detailed flow behaviors in this regime are beyond the interest of this study and thus are not pursued further in this work.

The behaviors of the separated flow varying with $L_s/\sqrt{(h_f U_0)}/f$ can be further studied from Fig. 3b, which shows the distributions of the intermittency function I_r , obtained at different $L_s/\sqrt{(h_f U_0)}/f$ values for $K = 0.005$, $h_f/h_s = 0.67$, and $U_0 = 4 \text{ m/s}$. This figure shows that, when $L_s/\sqrt{(h_f U_0)}/f = 1.34$, which is greater than the value of 1.22 , the shape of the distribution is similar to that of an ordinary backward-facing step, except for a shift of ΔX_r . When $L_s/\sqrt{(h_f U_0)}/f = 0.67$, although the reattachment length defined as a streamwise distance from $X = 0$ to the location where $I_r = 50\%$ is less than the reattachment length of an ordinary backward-facing step, the region in which the I_r value is less than 1.0 is, in fact, enlarged. This corresponds to a situation in which when the oscillating fence approaches the upper dead point, the vortical structure developed behind the oscillating fence extends over the step. As a result, the effective height of the step increases at these moments, as does the instantaneous reattachment length. When $L_s = 0$, the distribution appears to be quite flattened, and the location corresponding to $I_r = 50\%$ cannot be determined accurately.

Effect of K

Variations of $-\Delta X_r/X_r$ vs K for a number of cases studied are shown in Fig. 4a, in which two distinct regions can be identified. In the region of K larger than $K_{cr} = 0.009$, $-\Delta X_r/X_r$ increases almost linearly with K for each of the cases studied. The maximum reduction is seen to be due to the case

of $L_s/h_s = 4$, $h_f/h_s = 0.8$, and $U_0 = 4$ m/s, which amounts to 42%. Following the trend shown, one expects that higher reduction of the reattachment length would be possible if the reduced frequency could be increased over 0.06. Unfortunately, such experiments were not possible in the present study, due to the limitation of the setup. It is also expected that the reduction should level off at some higher K values. Nagib et al.¹⁴ and Reisenthal et al.¹⁵ explored flow characteristics in this respect by increasing the nondimensional frequency of a flapping spoiler immersed in the separation region behind a backward-facing step up to 0.12.

When K is less than K_{cr} , $-\Delta X_r/X_r$ varies more drastically than that in the region of K being larger than K_{cr} . Interestingly, for some cases of K values considerably less than K_{cr} , the corresponding $-\Delta X_r/X_r$ values are not necessarily negative. Since under these circumstances an organized vortical structure does not develop behind the oscillating fence, this appearance implies that the mechanism associated with the effect of streamline curving, mentioned previously for the fixed-fence cases in Fig. 2, is at work. It is also found in the figure that for the case of $L_s = 0$ the $-\Delta X_r/X_r$ values obtained are negative even though the reduced frequency is higher than the critical value.

Smoke visualization pictures obtained for the case of $K > K_{cr}$ and the case of $K < K_{cr}$ are shown in Figs. 4b and 4c, respectively, which reveal marked differences. For $K > K_{cr}$ (Fig. 4b) the vortical structure generated by the oscillating fence is seen to interact strongly with the flow behind the step. The remarkable finding is that, at $t/T = 3/4$, the flow in the region immediately behind the step appears as an organized vortical structure situated beneath the main vortical structure; at a latter instant, $t/T = 0$, these two flow structures of the same rotating sense apparently merge. This sequence of pictures illustrate that the vortical structure generated by the oscillating fence upstream has a predominant effect on flow behind the backward-facing step. More discussion on the evolution process of this flow will be given later with the assistance of phase-averaged velocity measurements results

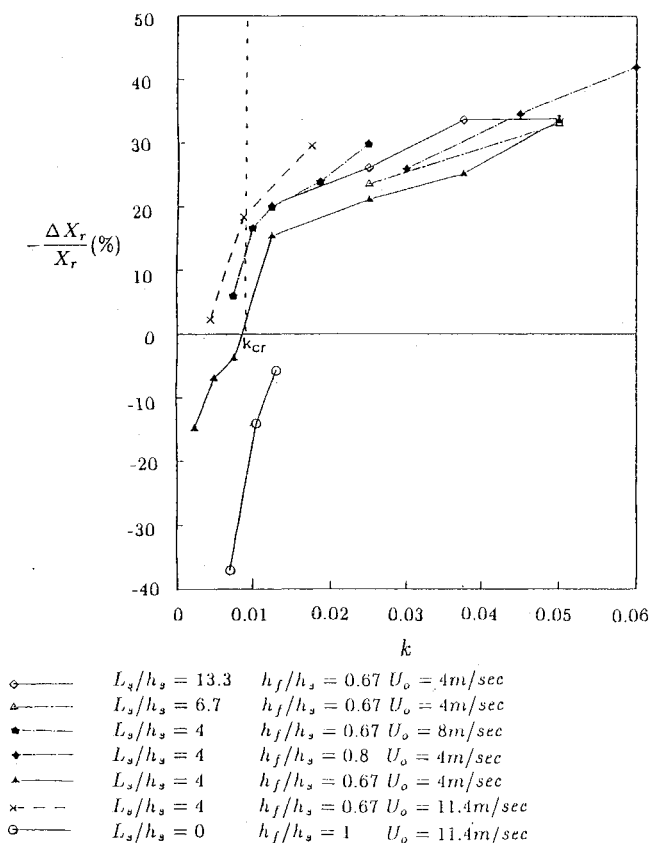


Fig. 4a Diagram of $-\Delta X_r/X_r$ vs K .

(Fig. 7). For $K < K_{cr}$ (Fig. 4c) no vortical structure is seen behind the oscillating fence at any instant. Rather, the shear layer shed from the edge of the fence flap up and down in response to the motion of the fence and affects the downstream region in a quasisteadily fashion. Coincidentally, the picture of $t/T = 1/4$ indicates that the shear layer reattaches to the wall immediately before the step, which results in a significant reduction of the separation region at this moment. This appearance resembles the picture seen in Fig. 2b of the case $h = 5$ mm and $f = 0$.

Effect of h_f/h_s

Three sets of the data obtained at $h_f/h_s = 0.25$, 0.67, and 0.8, respectively, for different K values while $L_s = 4h_s$ are plotted in Fig. 5. The dashed lines included in the figure, drawn by linear interpolation of the available data points, indicate the trends of $-\Delta X_r/X_r$ varying with h_f/h_s , at constant K values. This figure suggests that, the higher the value of h_f/h_s , the more effective the suppression of the separation region behind the backward-facing step. It should be mentioned that in the present study the h_f/h_s values chosen are below 1.0.

Effect of Re_θ

Variations of the time-mean reattachment lengths measured X_r against the Reynolds numbers for a case of $f = 15$ Hz, $h_f/h_s = 0.67$, and $L_s = 4h_s$, are shown in Fig. 6. Also included in this figure for comparison are two curves corresponding to the cases of an ordinary backward-facing step without and

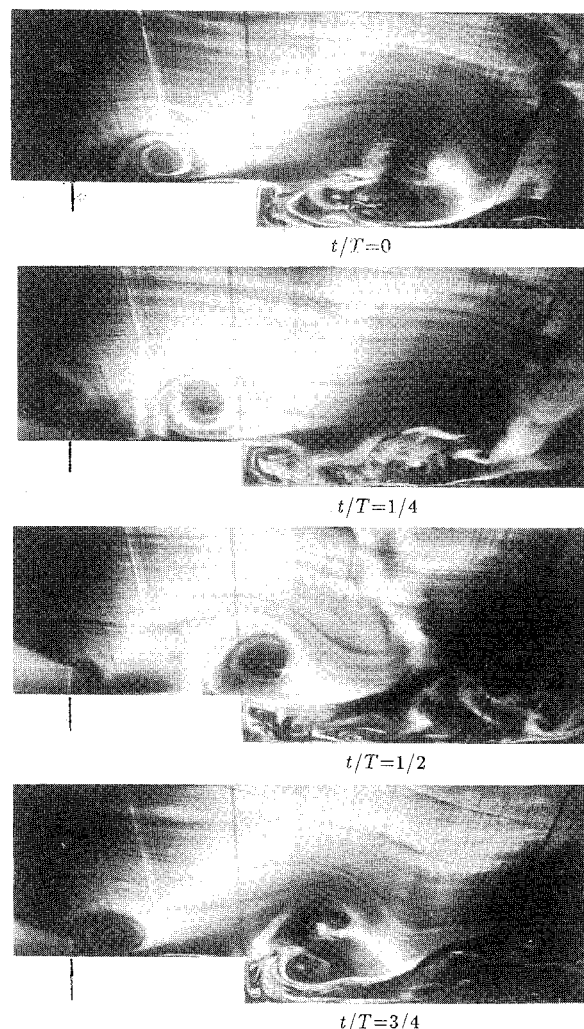


Fig. 4b Smoke visualization pictures for $(K, h_f/h_s, L_s/h_s, U_0) = (0.1, 0.67, 4, 0.5 \text{ m/s})$.

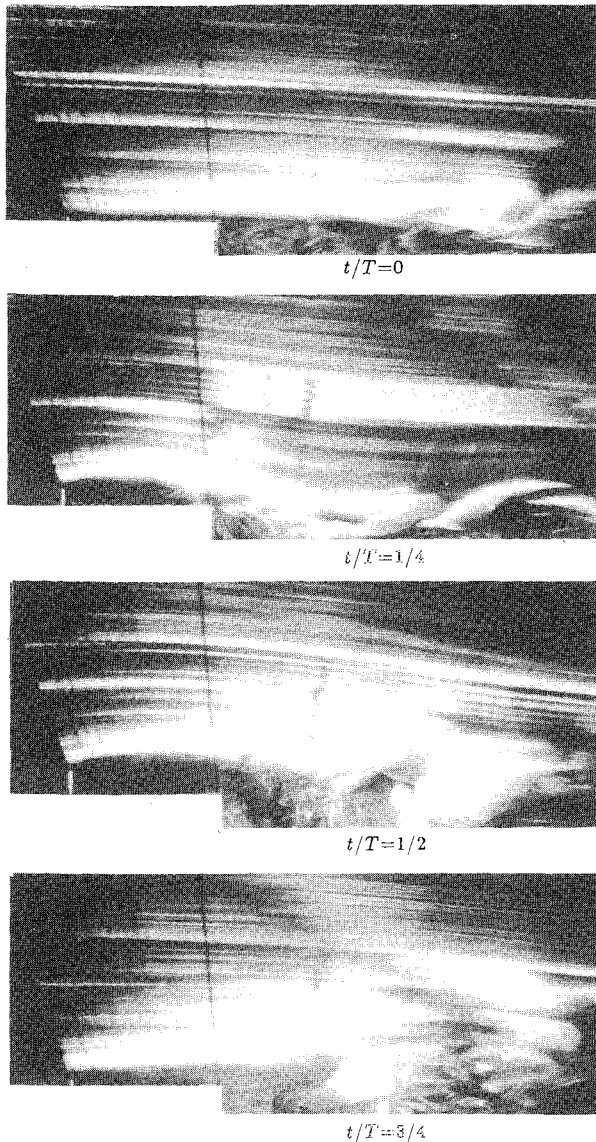


Fig. 4c Smoke visualization pictures for $(K, h_f/h_s, L_s/h_s, U_0) = (0.005, 0.67, 4, 1 \text{ m/s})$.

with the trip device placed upstream, denoted as the reference cases 1 and 2, respectively. First of all, it is seen that with the presence of the oscillating fence the reattachment length measured is weakly dependent on the Reynolds number in the range studied of 250–1350. This appearance strongly suggests that the artificial disturbance introduced by the oscillating fence is too strong to be affected by the characteristics of the upstream boundary layer. Moreover, a trend noted is that X_r'/h_s increases slightly with Re_θ when Re_θ is greater than 700. This is attributed to the fact that the values of $L_s/\sqrt{(h_f U_0)/f}$ for these Reynolds numbers are less than 1.22 as indicated in Fig. 3a.

For reference case 1 the reattachment length decreases with the Reynolds number in the range of 140–200, signifying that a transition process occurred in the separated layer before it reattached to the wall surface.³ The Reynolds numbers corresponding to this transition range are noticed to be lower than the Reynolds numbers reported by Eaton and Johnston.³ This discrepancy could be attributed to the intrusion of the split-film probe in the flowfield.

For reference case 2 the reattachment length measured appears to be lower at Reynolds numbers between 280 and 700. A speculation for this behavior is that in this Reynolds number range the disturbances generated by the trip device upstream have not developed fully turbulently at the step, more or less

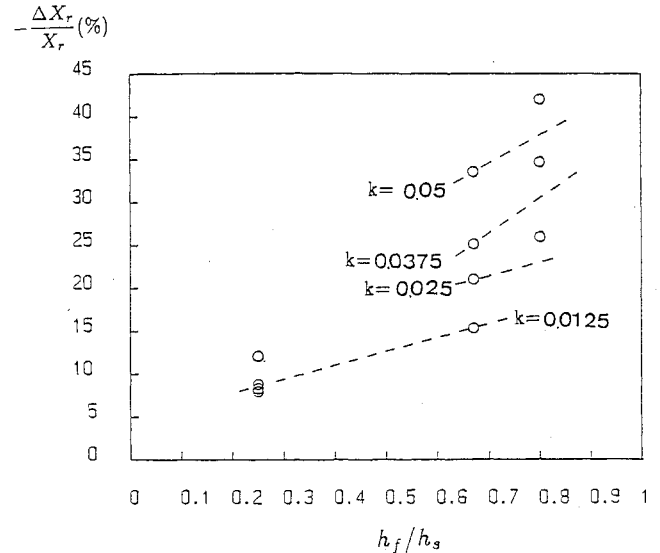


Fig. 5 Diagram of $-\Delta X_r/X_r$ vs h_f/h_s for $(L_s/h_s, U_0) = (4, 4 \text{ m/s})$.

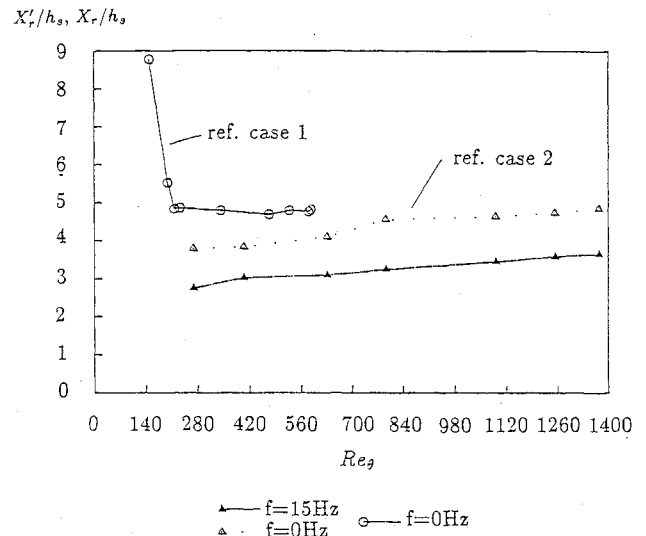


Fig. 6 Diagram of the reattachment length measured for $(f, h_f/h_s, L_s/h_s) = (15 \text{ Hz}, 0.67, 4)$ against Re_θ . Reference case 1: without trip device upstream; reference case 2: with trip device upstream.

exited in a form of larger scale structures. Conceivably, these disturbances would transport momentum more effectively and result in a reduction in the reattachment length. At higher Reynolds numbers, the boundary layer at the step becomes turbulent and the reattachment length measured approaches an asymptotic value.

Evolution of the Flowfield at $K > K_{cr}$

Insights into the evolution process of the unsteady flow at $K > K_{cr}$ can be gained from an experiment that surveyed the flowfield with a split-film probe. The velocity data obtained were reduced with a phase-averaging technique that gave the spatial distribution of the velocity field referring to a specific phase of the oscillation of the fence. For each measured point the ensemble-averaging process was performed for a collection of 100 samples. Mathematically, this process is expressed as follows:

$$\langle U(\phi) \rangle = \frac{1}{n} \sum_{i=1}^n U(iT + \phi); \quad n = 100 \quad (7)$$

Accordingly, the phase-averaged fluctuation in the streamwise component, denoted as $\langle u \rangle$, is given by

$$\langle u \rangle = \langle U \rangle - \bar{U} \quad (8)$$

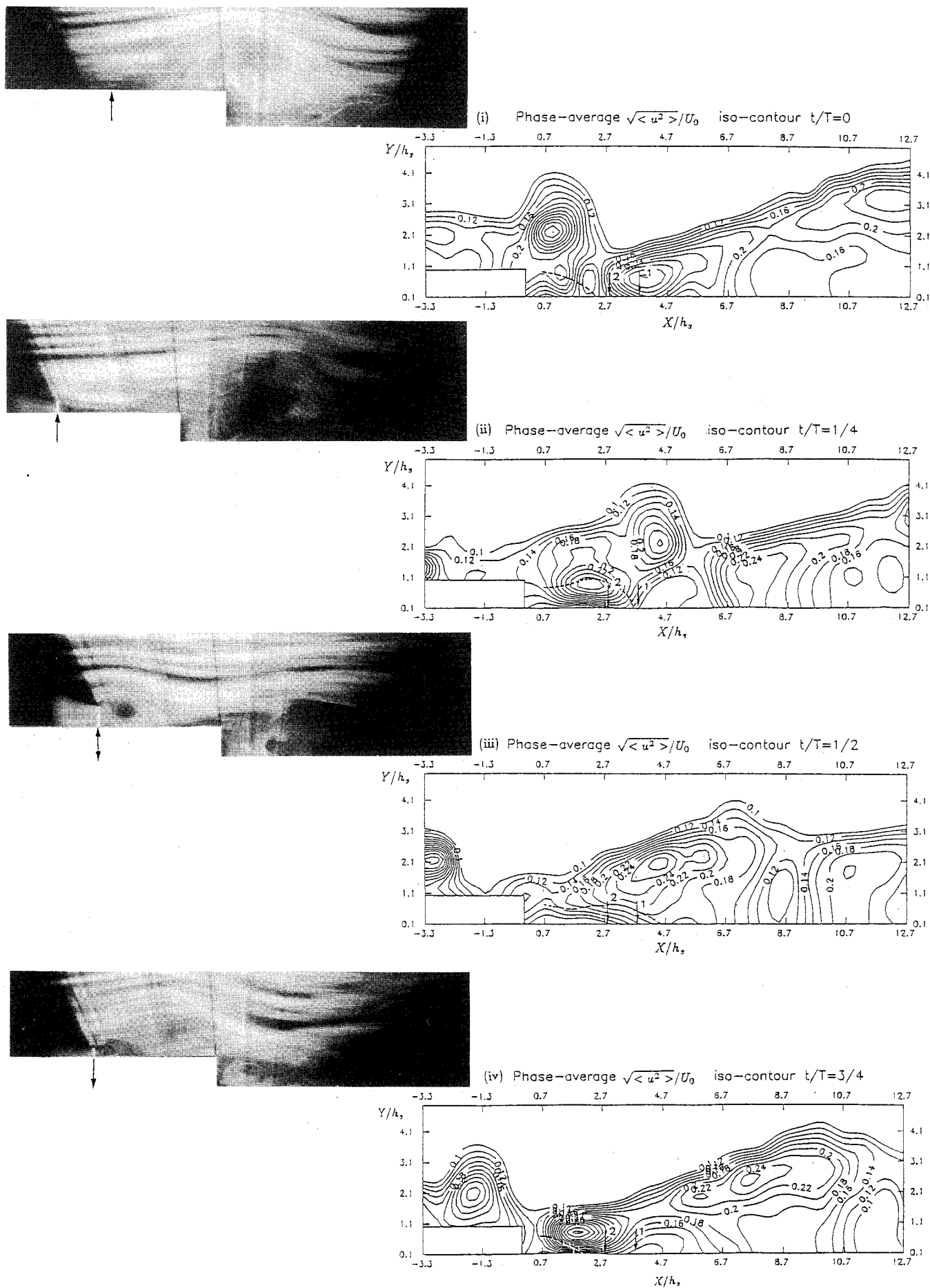


Fig. 7a The $\sqrt{\langle u^2 \rangle}/U_0$ contour diagrams and the smoke visualization pictures. Reference case 1: reattachment point of an ordinary backward-facing step flow; reference case 2: time-mean reattachment point of this case.

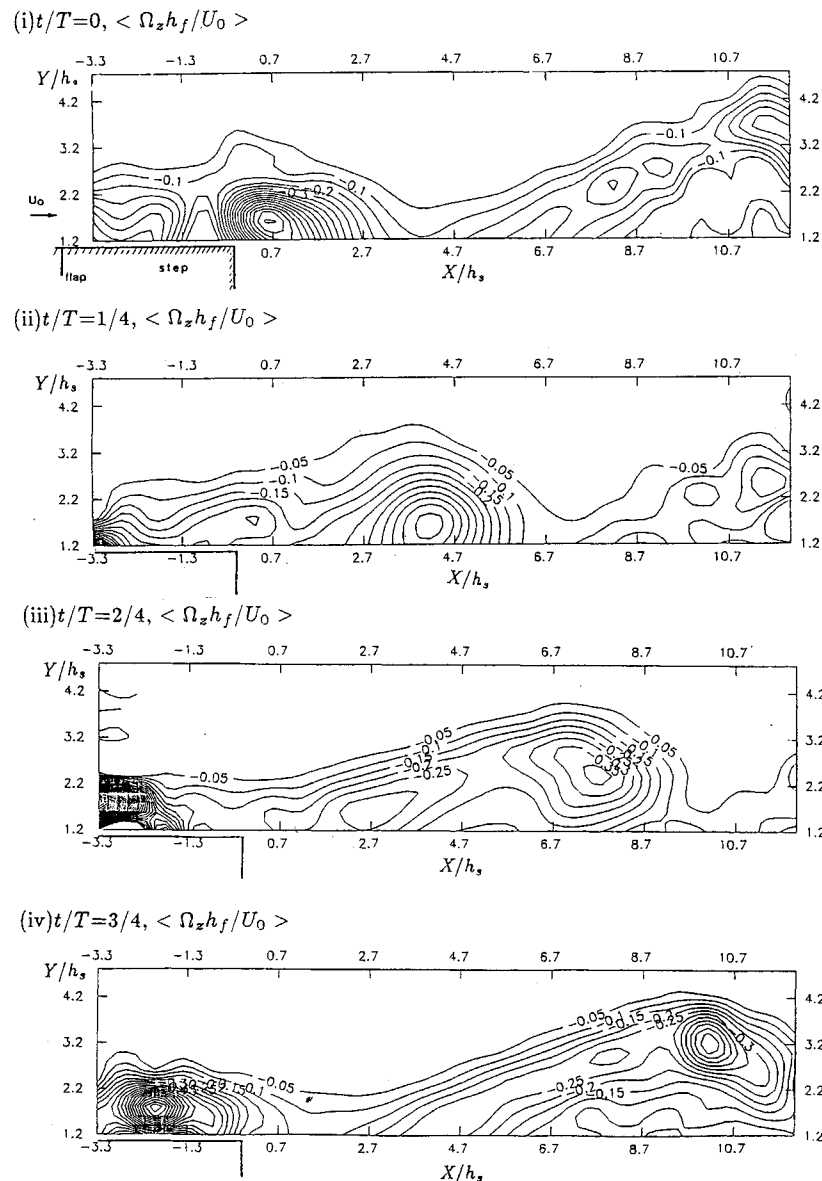


Fig. 7b Ensemble-averaged vorticity contour diagrams: $(K, h_f/h_s, L_s/\sqrt{(h_f U_0)/f}, U_0) = (0.0375, 0.67, 1.16, 4 \text{ m/s})$.

Although the split-film measures the component of the streamwise velocity only, Koga⁶ pointed out that the phase-averaged streamwise turbulence energy distribution could qualitatively simulate the appearance of large-scale structure in the flowfield (see also Reisenthal et al.¹⁵). This similarity is also confirmed by the experimental results shown in Fig. 7, which compares the $\sqrt{\langle u^2 \rangle}/U_0$ distributions obtained by the split-film probe, the smoke visualizations, and the phase-averaged vorticity distributions obtained by the cross-type hot-wire, at $K=0.0375$, $h_f/h_s=0.67$, $L_s/\sqrt{(h_f U_0)/f}=1.16$, and $U_0=4 \text{ m/s}$. The reason behind this similarity is that the ensemble-averaged velocity fluctuations basically reveal the passage of the repeatable organized flow structures; therefore, the region of high intensity in $\sqrt{\langle u^2 \rangle}/U_0$ should coincide with the occurrence of the vortical structure.

The $\sqrt{\langle u^2 \rangle}/U_0$ diagrams shown in Fig. 7a give the phase-averaged flow structures at $t/T=0, 1/4, 1/2$, and $3/4$, respectively. In this figure the instantaneous smoke visualizations taken at the corresponding time instants are also provided for comparison, which confirms that the present phase-averaging technique is valid. The dashed line marked in each of the $\sqrt{\langle u^2 \rangle}/U_0$ diagrams indicates the boundary of reverse flow behind the backward-facing step, on which the streamwise velocity measured is zero. Comparing the dashed lines shown in the four diagrams, one realizes that the size of

the reverse-flow region varies with time. For reference, the streamwise location of $X=X_r$, and the time-mean reattachment point for this case are also marked on the horizontal axis by the \downarrow symbols with 1 and 2, respectively.

It is instructive to study the evolution of the flow from the $\sqrt{\langle u^2 \rangle}/U_0$ contour diagrams in Fig. 7a and the phase-averaged vorticity contours in Fig. 7b. At $t/T=0$, the vortical structure convects right above the step. The downwash motion induced by this flow structure apparently extends to the region behind the step and influences the flow near the wall in a reverse direction. The other flow structure situated further downstream, seen in the $\sqrt{\langle u^2 \rangle}/U_0$ diagram, is identified to be the one formed behind the step at an earlier moment [see also the $\sqrt{\langle u^2 \rangle}/U_0$ diagram at $t/T=3/4$ (Fig. 7a(iv))]. Comparing the flow structures seen in the diagrams of $t/T=0$ and $1/4$, one can further estimate the convection speed of the artificially generated vortical structure to be about $0.8U_0$, while the reverse-flow region behind the step is enlarged at a lower speed. The reverse flow behind the step appears to rotate in the same sense as the artificially generated vortical structure. Therefore, these two flow structures have a tendency to merge at following time instants. This development is confirmed by the appearance of the $\sqrt{\langle u^2 \rangle}/U_0$ diagram at $t/T=1/2$. A similar appearance is also noted in Fig. 4b(i). This merging process further enlarges the reverse-flow region

to an extent larger than the time-averaged size. At this moment, one also notices that in the region upstream of the step a vortical structure behind the oscillating fence grows to about its maximum size. By the time $t/T = 3/4$, this vortical structure has been released downstream and is convecting toward the step. On the other hand, downstream of the backward-facing step, the merged flow structure has shed away from the step, like the process of vortex shedding from a bluff body, and a renewed vortical structure is formed behind the step. The renewed growth of the vortical structure behind the step bears a resemblance to the situation of an impulsive flow over the step.¹⁶ It is also noticed that the behavior of vortex shedding behind a backward-facing step is not uniquely found in the present flow. Mullin et al.¹⁷ observed that if the freestream velocity varied sinusoidally over a step at a nondimensional frequency of 0.007, based on the mean freestream velocity and the step height, the shedding of the vortex behind the step occurred at the moment when the retardation of the freestream velocity was a maximum.

The preceding observations suggest that suppression of the reverse-flow region behind a backward-facing step is mainly due to the downwash motion induced by the vortical structure. The sequence is that as the vortical structure convects over the step it sweeps away the low-speed fluid behind the step, then subsequently induces another vortical structure in reverse flow. The induced vortical structure will merge with the artificially generated vortical structure at later instants.

These experimental observations lead to a postulation that the reduction of the time-mean reattachment length should be proportional to the number of vortical structures per unit time convecting over the backward-facing step. This argument seems to be in good agreement with the appearance seen in Fig. 4a that $-\Delta X_r/X_r$ is linearly proportional to K , when $K > K_{cr}$.

Conclusions

The parameters of the oscillating fence relevant to the control of separated flow behind a backward-facing step have been studied in this work. The conclusions obtained are as follows.

1) When $K > K_{cr}$, the distance from the oscillating fence to the step, in terms of $L_s/\sqrt{(h_f U_0)/f}$, should be larger than 1.22, allowing a complete formation of the unsteady vortical structure before the step. As long as this condition is satisfied, $-\Delta X_r/X_r$ is weakly dependent on this parameter.

2) When $0.06 > K > K_{cr}$, $-\Delta X_r/X_r$ increases linearly with K . The maximum reduction obtained in the present study exceeds 40%.

3) In the range of $h_f/h_s < 1$, $-\Delta X_r/X_r$ increases with h_f/h_s while K is held constant.

4) No appreciable effect on $\Delta X_r/X_r$ is found when R_{θ} is varied in the range of 250–1450, as $K > K_{cr}$.

5) The phase-averaged velocity measurements obtained for $K > K_{cr}$ show that suppression of the reverse-flow region behind the step is mainly due to the downwash motion induced by the artificially generated vortical structure. The flowfield is characterized by the interaction of the vortical structures generated by the oscillating fence upstream and the flow behind the step. The reverse flow developing behind the step is, in effect, a portion of a well-organized vortical structure that convects downstream every cycle of the oscillating motion of

the fence, through a process of merging with the artificially generated vortex and then shedding away from the step.

Acknowledgments

Financial support from the National Science Council, Contract NSC-77-0401-E 006-38, Republic of China, for this work is gratefully acknowledged. J. J. Miao and K. C. Lee thank C. M. Ho of the University of Southern California, for discussions regarding this work.

References

- ¹Miao, J. J., Chen, M. H., and Chou, J. H., "Frequency Effect of an Oscillating Plate Immersed in a Turbulent Boundary Layer," AIAA Paper 89-1016, March 1989.
- ²Miao, J. J., Chen, M. H., and Chou, J. H., "Flow Structure of a Vertically Oscillating Plate Immersed in a Flat-plate Turbulent Boundary Layer," *Proceedings of the 11th Symposium on Turbulence*, University of Missouri, Rolla, Oct. 1988.
- ³Eaton, J. K., and Johnston, J. P., "A Review of Research on Subsonic Turbulent Flow Reattachment," *AIAA Journal*, Vol. 19, No. 12, 1981, pp. 1093–1100.
- ⁴Kim, J., Kline, S. J., and Johnston, J. P., "Investigation of a Reattaching Turbulent Shear Layer: Flow over a Backward-Facing Step," *Journal of Fluids Engineering*, Vol. 102, Sept. 1980, pp. 302–308.
- ⁵Roos, F. W., and Kegelmann, J. T., "Structure and Control of Flow over a Backward-Facing Step," *Forum on Unsteady Flow Separation*, edited by K. N. Ghia, Fluids Engineering Division, American Society of Mechanical Engineers, New York, 1987, pp. 215–223.
- ⁶Koga, D. J., "Control of Separated Flowfields Using Unsteadiness," Ph.D. Dissertation, Illinois Institute of Technology, Chicago, 1983.
- ⁷deBrederode, V., and Bradshaw, P., "Three-Dimensional Flow in Nominally Two-Dimensional Separation Bubbles. I. Flow Behind Rearward-Facing Step," Imperial College, Aeronautical Rept. 72-19, 1972.
- ⁸Chen, M. H., "A Vertically Oscillating Plate Immersed in a Flat-Plate Turbulent Boundary Layer," Ph.D. Dissertation, Institute of Aeronautics and Astronautics, National Cheng-Kung University, Tainan, Taiwan, 1989.
- ⁹Eaton, J. K., Westphal, R. V., and Johnston, J. P., "Two New Instruments for Flow Direction and Skin Friction Measurements in a Separated Flow," *ISA Transactions*, Vol. 21, No. 1, 1981, pp. 69–78.
- ¹⁰Westphal, R. V., Eaton, J. K., and Johnston, J. P., "A New Probe for Measurement of Velocity and Wall Shear Stress in Unsteady, Reversing Flow," *Journal of Fluids Engineering*, Vol. 103, Sept. 1981, pp. 478–482.
- ¹¹Good, M. C., and Joubert, P. N., "The Form Drag of Two-Dimensional Bluff-Plates Immersed in Turbulent Boundary Layer," *Journal of Fluid Mechanics*, Vol. 31, Part 3, 1968, pp. 547–582.
- ¹²Francis, M. S., Keese, J. E., Lang, J. D., Sparks, G. W., Jr., and Sisson, G. E., "Aerodynamic Characteristics of an Unsteady Separated Flow," *AIAA Journal*, Vol. 17, No. 12, 1979, pp. 1332–1339.
- ¹³Reynolds, W. C., and Carr, L. W., "Review of Unsteady, Driven, Separated Flows," AIAA Paper 85-0527, March 1985.
- ¹⁴Nagib, H., Reischenthal, P. R., and Koga, D. J., "On the Dynamical Scaling of Forced Unsteady Separated Flows," AIAA Paper 85-0553, March 1985.
- ¹⁵Reischenthal, P. H., Nagib, H. M., and Koga, D. J., "Control of Separated Flows Using Forced Unsteadiness," AIAA Paper 85-0556, 1985.
- ¹⁶Durst, F., and Pereira, J. C. F., "Time-Dependent Laminar Backward-Facing Step Flow in a Two-Dimensional Duct," *Journal of Fluids Engineering*, Vol. 110, Sept. 1988, pp. 289–296.
- ¹⁷Mullin, T., Greated, C. A., and Grant, I., "Pulsating Flow over a Step," *Physics of Fluids*, Vol. 23, April 1980, pp. 669–674.